The promotion effects of Ba on manganese oxide for CH_4 deep oxidation

Xiang Wang [*] and You-chang Xie

Institute of Physical Chemistry, Peking University, Beijing 100871, PR China
E-mail: wangx2@seas.upenn.edu

Received 8 September 2000; accepted 12 December 2000

A series of catalysts based on high specific surface area MnO_2 precursor and modified by various amount of Ba were prepared and applied in CH_4 deep oxidation. The catalysts were characterized by means of N_2-BET, XRD, TG-DTA, H_2-TPR and CH_4-TPR techniques. The catalytic evaluation results show that CH_4 oxidation activity of the modified catalysts was enhanced, with the optimal Ba/Mn mol ratio being ~0.1. Whereas, comparative study demonstrates that CO oxidation activity of the modified catalysts was not improved. It was shown previously that the reactivity of the oxygen species in a catalyst is crucial for CO oxidation, but not critical for CH_4 oxidation. In this study, TPR results verify that the mobility and reactivity of the lattice oxygen of Ba-modified catalysts is not improved, thus leading to no enhancement of their CO oxidation activity. However, the addition of Ba into manganese oxides is supposed to improve the basicity of the lattice O^{2-} of the prepared catalysts, which is favorable for the rupture of the first C–H bond in CH_4, the rate-determining step of the reaction. It is thus concluded that the enhanced CH_4 oxidation activity of the modified catalysts can be attributed to this modification effect of Ba.

KEY WORDS: CH_4 deep oxidation; CO oxidation; manganese oxide catalysts; Ba additive

1. Introduction

CH_4, the main component of natural gas, is an attractive fuel due to its low carbon to hydrogen ratio and the easy availability of natural gas around the world [1–3]. However, CH_4 is also found to be a potent greenhouse gas [1,2,4]. Though the emission of CH_4 is not regulated at present, it is expected to be restricted in the near future [1,3].

Low-temperature deep oxidation of CH_4 is an effective way to utilize it as an energy source, or prevent it from polluting the atmosphere. Since the 1970s, catalysts based on precious metals such as Pt, Pd and Rh have been successfully developed and applied in hydrocarbon combustion [5,6]. However, these conventional catalysts are not active enough for applications in low-temperature CH_4 oxidation [2,3]. Presently, it is still a challenge and an important research topic to find an effective and applicable catalyst for this process.

CH_4 is known to be the most difficult to oxidize among all the hydrocarbons, since it contains only very strong C–H bonds. In general, the rupture of the first C–H bond is crucial and considered as the rate-determining step in CH_4 oxidation reactions [7–13]. Supported Pd is the most active catalyst for CH_4 oxidation due to the superior ability of Pd to activate both C–H and O–O bond [14]. However, this class of catalysts have still some limitations, e.g., the strong inhibition of their activity by the reaction products (CO_2 and H_2O) [9–11], the limited availability [15] and high price of Pd. Therefore, over recent years, people have paid considerable attention to basic metal oxides, expecting to achieve some stable and active catalysts, which have the potential to be practically applied in CH_4 deep oxidation. Manganese oxides are highly active catalysts for CO oxidation [16–20] and hydrocarbon combustion [21,22], and have been extensively studied in these two processes as well as for many other reactions [23,24]. Because of their easy availability, environment-friendly characteristics and remarkable redox property, they are latent and attractive combustion catalysts, and worth trying for CH_4 deep oxidation.

When studying oxidative coupling of CH_4, Campbell et al. [13] found that the relative activity of rare-earth metal oxides parallels their basicity. Burch et al. [8] suggested that the efficient activation of CH_4 requires highly basic sites. The addition of barium oxide into manganese oxides has been reported to increase the basicity of the obtained catalysts [25]. Therefore, based on these interesting previous studies, our objective in the present work is investigating the modification effects of Ba on manganese oxide for CH_4 deep oxidation, expecting to find some promising catalysts. As an attempt to elucidate the nature of the active sites, CO oxidation was also carried out over the modified and unmodified catalysts.

2. Experimental

2.1. Catalyst preparation

The high specific surface area MnO_2 precursor (265 m^2/g) was prepared via the stoichiometric reaction between

---

[*] To whom correspondence should be addressed. Current address: Department of Chemical Engineering, Towne Building, Room 311A, University of Pennsylvania, 220 South 33rd Street, Philadelphia, PA 19104, USA.

1011-372X/01/0300-0051$19.50/0

$KMnO_4$ and $Mn(NO_3)_2$ solutions, similar to the methods reported in [26,27]. Typically, 0.24 M $KMnO_4$ solution was dripped into 50% $Mn(NO_3)_2$ that was under stirring. A brown precipitate, which has been proven to be α-MnO_2 fine powder [28], was formed promptly. When the reaction was finished, the pH of the mixture is ~2.0. The mixture was then vacuum filtered and washed repeatedly with distilled water, until the water passing through the precipitate was neutral. Afterwards, it was dried at 110 °C overnight, and used as the precursor to prepare the catalysts.

Ba–Mn binary oxide catalysts with different Ba/Mn mol ratios (0.05, 0.10, 0.15, 0.20, 0.25 and 0.30) were prepared via impregnating a calculated amount of $Ba(NO_3)_2$ aqueous solution onto the MnO_2 precursor. After evaporation to dryness in a water bath, all the samples were calcined in static air atmosphere at 600 °C for 4–6 h. The catalysts are denoted by the names of the metal elements and the corresponding Ba/Mn mol ratio, such as BaMn0.05, BaMn0.10, BaMn0.15, BaMn0.20, BaMn0.25 and BaMn0.30. The unmodified MnO_x catalyst was prepared by direct calcination of the MnO_2 precursor under the same conditions.

2.2. Catalyst characterization

BET surface areas were measured by nitrogen adsorption–desorption at 77 K with a ST-30 instrument.

XRD patterns were recorded on a BD-90 X-ray diffractometer with Cu K_α radiation of 40 kV and 20 mA and a Ni filter. The scan step is 0.1° with a preset counting time of 4 s; and the scan region is from 10° to 70°.

TG-DTA analyses were performed in airflow using a Dupont 1090 instrument, starting from room temperature to 1100 °C with a ramp of 15 °C/min.

H_2-TPR was carried out using a H_2/N_2 (5.1%) gas mixture, the temperature being increased from room temperature to 800 °C with a rate of 10 °C/min. Prior to entering into the catalyst bed, the gas flow was purified with a MnO oxygen trap and a molecule sieve 5A H_2O trap. Another water trap was equipped at the outlet of the reactor to remove the formed water. A thermal conductivity detector (TCD) was used to monitor the H_2 consumption. In some cases, the amount of consumed H_2 was calibrated with $CuO + SiO_2$ standard. Generally, the catalysts were diluted with quartz powder to ~10 wt%. 100 mg mixture containing ~10 mg pure catalyst powder was used for the H_2-TPR experiment.

CH_4-TPR was performed using a CH_4/N_2 (5.5%) gas mixture on the similar set-up to H_2-TPR with nearly the same methods and experiment conditions. In this experiment, the main reaction products are H_2O and CO_2; the formation of CO is negligible, as also testified by Stobbe et al. [29]. We got information via measuring the consumption of CH_4. To rule out the effect of formed CO_2 on the signal, compared with the H_2-TPR set-up, an additional molecule sieve 5A trap was equipped at the outlet of the reactor to adsorb CO_2. In case this trap is saturated by CO_2, the baseline is noisy and some negative CO_2 peaks can be observed. With this method, we make sure that the obtained profiles are really based on CH_4 consumption, and not perturbed by the formed CO_2.

2.3. Activity evaluation

Catalytic tests were carried out in a U-shaped fixed-bed microreactor (ID = 6 mm) with a continuous downflow. The samples were pressed under 8 MPa for 2 min to form pellets, and then crushed and sieved. Typically, 0.2 ml 40–60 mesh catalysts were used for activity evaluation. To avoid channeling, ~1 ml same size porcelain particles were loaded above the catalyst bed. A blank experiment showed the lack of activity of the porcelain particles at the reaction temperature region. A K-type thermocouple was placed on top of the catalyst bed (touch the catalyst) to monitor the reaction temperature. To measure the light-off behaviors of the catalysts, all data were collected with increasing temperature. The volume composition of the feed gas is CH_4 1.5%, O_2 18% and balanced by high purity N_2. The total feed flow rate was 70 ml/min corresponding to a gas hourly space velocity (GHSV) 21 000 h^{-1}. The reactants and products were analyzed with an on-line 1102G GC equipped with a TCD on a Porapak Q column for CH_4 and CO_2, and on a molecule sieve 5A column for CH_4 and CO. Before analysis, the reaction at each temperature over all the studied catalysts was stabilized at least 30 min. The flow rate of the carrier gas He is 30 ml/min. CH_4 conversion was calculated by the change of its peak area before and after the catalyst bed.

CO oxidation was performed on the same set-up. Typically, 0.2 ml 40–60 mesh catalysts were evaluated at a GHSV 21 000 h^{-1} with increasing temperature. The volume composition of the feed gas is 2.5% CO in air. The conversion of CO was calculated by the change of its peak area before and after the catalyst bed.

3. Results

3.1. Activity evaluation

3.1.1. CH_4 deep oxidation

Figure 1 shows the typical light-off behavior of CH_4 over unmodified MnO_x and Ba-modified BaMn0.10. Obviously, the addition of Ba enhances the activity of manganese oxide toward CH_4 oxidation, especially at relatively lower conversion level. CH_4 complete oxidation over MnO_x takes place at 580 °C, while that over BaMn0.10 occurs at 540 °C. Both catalysts were subjected to 10 h durability test at their corresponding complete CH_4 oxidation temperature; no deactivation was found.

The steady-state CH_4 oxidation rates over the modified and unmodified catalysts are compared in figure 2 as Arrhenius plots. It is obvious that the activity of BaMn0.10 is much higher than that of the unmodified MnO_x, as evidenced by its much higher reaction rates. The apparent activation energy on MnO_x and BaMn0.10 is 84 and 94 kJ/mol, respectively.

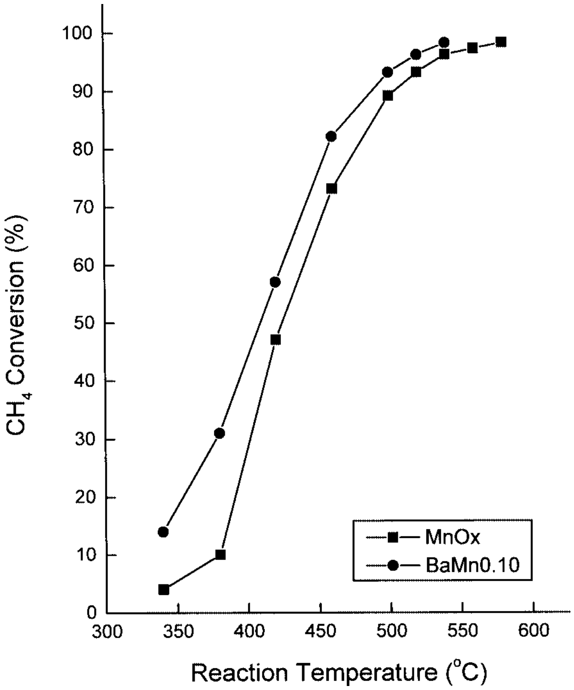

Figure 1. CH_4 deep oxidation over unmodified MnO_x and Ba-modified BaMn0.10 catalyst.

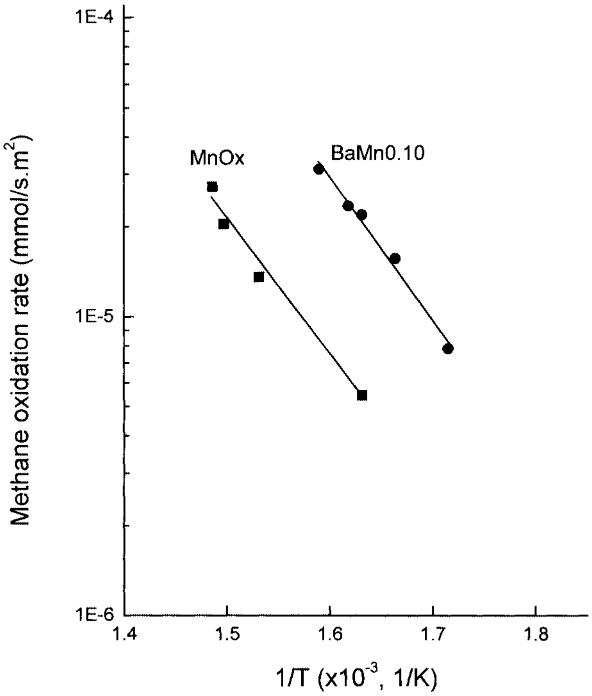

Figure 2. Arrhenius plots for CH_4 deep oxidation over unmodified MnO_x and Ba-modified BaMn0.10.

The effects of Ba loading on the reactivity of the catalysts were explored. T_{10} and T_{98}, the temperatures corresponding to 10 and 98% CH_4 conversion, are plotted against Ba/Mn mol ratio in figure 3. The T_{10} and T_{98} over MnO_x are 380 and 580 °C, respectively. All the modified catalysts exhibit lower T_{10} than the unmodified MnO_x, with the lowest T_{10} (325 °C) being achieved over BaMn0.05. The neighbor catalyst, BaMn0.10 shows similar T_{10} (330 °C), which also displays the lowest T_{98} (540 °C) among all the catalysts. When Ba/Mn ratio is above 0.20, the complete oxidation activity of the catalysts is degraded, as testified by their higher T_{98}. Apparently, the addition of not too much Ba can enhance the activity of manganese oxide toward CH_4 deep oxidation, with the optimal Ba/Mn mol ratio around 0.1.

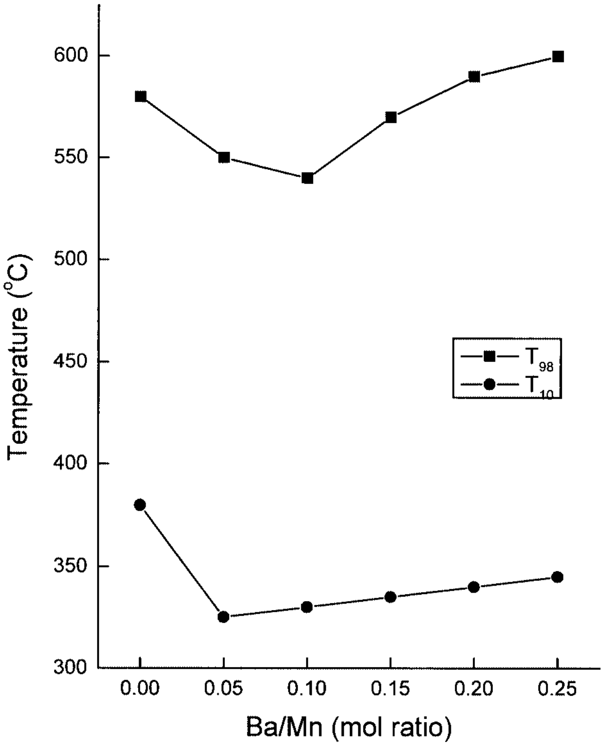

Figure 3. The effects of Ba loading on the reaction performance of the catalysts.

3.1.2. CO oxidation

To understand and unravel the possible reasons leading to the improved activity for CH_4 oxidation of manganese oxide via Ba addition, CO oxidation over MnO_x and BaMn0.10 were also carried out for comparative study. Different from CH_4 oxidation, the results in figure 4 substantiate that BaMn0.10 exhibits nearly no promoted reaction performance when compared with the unmodified MnO_x. Both catalysts display almost the same activity and light-off behaviors, with the complete CO conversion occurring at 140 °C. It is noted here that the activation energy on MnO_x and BaMn0.10 is 41 and 46 kJ/mol, respectively, similar to what was found over manganese oxide catalysts by Imamura et al. [16].

3.2. BET surface areas and XRD measurements

BET surface areas of the catalysts are listed in table 1. All catalysts show much lower surface areas than the MnO_2 precursor (265 m^2/g), indicating that the MnO_2 precursor is metastable, which sintered and crystallized into more stable crystalline phases [28]. The surface area of MnO_x is

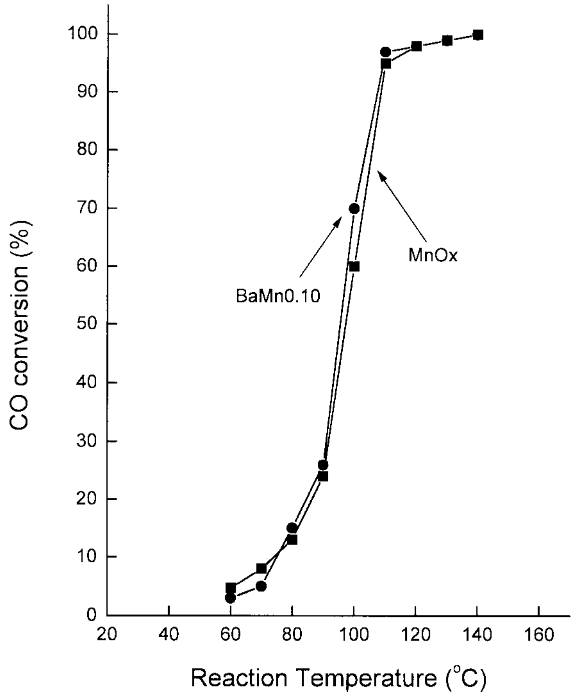

Figure 4. CO oxidation over unmodified MnO_x and Ba-modified BaMn0.10 catalyst.

Table 1
Physical properties of the catalysts.

Catalyst	BET surface area (m^2/g)	Phase composition measured by XRD
MnO_x	23	α-Mn_2O_3, β-MnO_2
BaMn0.05	21	α-Mn_2O_3, β-MnO_2, $BaMn_8O_{16}$
BaMn0.10	20	α-Mn_2O_3, $BaMn_8O_{16}$, $BaMnO_3$
BaMn0.15	19	α-Mn_2O_3, $BaMn_8O_{16}$, $BaMnO_3$
BaMn0.20	18	α-Mn_2O_3, $BaMn_8O_{16}$, $BaMnO_3$
BaMn0.25	17	α-Mn_2O_3, $BaMn_8O_{16}$, $BaMnO_3$
BaMn0.40	13	α-Mn_2O_3, $BaMn_8O_{16}$, $BaMnO_3$, $Ba(NO_3)_2$

23 m^2/g, which is somewhat higher than that of the Ba-modified catalysts. Furthermore, with the increase of Ba loading, the surface areas of the catalysts tend to decrease gradually. This may be caused by blocking of the pores of manganese oxide by the new-formed Ba–Mn composite oxides (see XRD results), or due to the low surface areas of the Ba–Mn composite oxides themselves. In brief, the change of surface areas of the catalysts does not seem to play a key role for the promoted CH_4 oxidation of the Ba-modified catalysts.

XRD was used to analyze the bulk phase composition of the catalysts. The crystalline phases detected in each sample are listed in table 1. For comparative study, pure $Ba(NO_3)_2$ was calcined under the same conditions and subjected to XRD analysis. Interestingly, it is found that it did not decompose into barium oxide, since only intensive diffraction peaks of $Ba(NO_3)_2$ were observed in its XRD pattern (results not shown). Our previous study shows that the high surface area MnO_2 precursor consists mainly of α-MnO_2 ultrafine powder [28]. However, the main crystalline phase of MnO_x is α-Mn_2O_3 (Bixbyte), together with a trace amount of β-MnO_2. This indicates that the metastable MnO_2 precursor transformed mainly into more stable α-Mn_2O_3 during the 600 °C calcination, accompanying the decrease of the oxidation state of Mn from 4+ to 3+. BaMn0.05 shows nearly the same diffraction pattern to MnO_x, except that the intensity of α-Mn_2O_3 diffraction peaks is somewhat lower. This may imply that Ba reacted with the MnO_2 precursor to form a new crystalline phase $BaMn_8O_{16}$ with minute quantity, whose diffraction peaks overlap with those of β-MnO_2, and nearly escape the detection of XRD.

Interestingly, starting from BaMn0.10, another new-formed crystalline phase $BaMnO_3$, together with $BaMn_8O_{16}$ was obviously observed in the samples. Upon further increasing the Ba loading, the amount of $BaMnO_3$ rises, while that of $BaMn_8O_{16}$ is almost constant, as testified by the intensity of their diffraction peaks. In comparison, the amount of α-Mn_2O_3 decreases monotonically with the increase of Ba loading. This indicates that, though pure $Ba(NO_3)_2$ is very stable under the calcination conditions adopted in this study, it can react with the metastable MnO_2 precursor to form new Ba–Mn composite oxides at the expense of α-Mn_2O_3 formation. $Ba(NO_3)_2$ can only be detected when Ba/Mn mol ratio reaches 0.4, as evidenced by its two strongest diffraction peaks in the XRD profile of BaMn0.40 (table 1).

It is worth noting here that, due to the formation of $BaMnO_3$ and $BaMn_8O_{16}$, a considerable amount of Mn was stabilized at higher oxidation state as 4+ in the modified samples, instead of 3+ in the unmodified MnO_x. This may contribute to the enhanced CH_4 oxidation activity of the modified catalysts.

3.3. TG-DTA analysis

To clarify the effect of Ba addition on the thermal behavior of manganese oxide, the MnO_2 precursor and BaMn0.10 dried at 110 °C without further calcination at higher temperature were analyzed with the TG-DTA method. The profiles are shown in figure 5.

Three obvious weight loss steps in the TG curve of MnO_2 precursor are observed: (a) A weight loss of 6.9% from ambient temperature to 200 °C, which may correspond to desorption of chemically bound water [20,27]. In this temperature region, the phase transformation of metastable α-MnO_2, the main component of the MnO_2 precursor, into more stable β-MnO_2 and its further crystallization upon increasing the temperature are supposed to happen. The total effects of all these processes resulted in an exothermic peak at 209 °C in its DTA curve. (b) A weight loss of 6.2% in the temperature region of 520–600 °C, associated with an endothermic peak at 588 °C in the DTA curve. This is generally assigned to the following process: $2MnO_2 \rightarrow Mn_2O_3 + \frac{1}{2}O_2$ [20,27,29]. (c) A weight loss of 0.9% around 900 °C, which is ascribed to the $Mn_2O_3 \rightarrow Mn_3O_4$ transformation [27,30]. A corresponding endothermic peak appears at the same temperature. However, another obvious endothermic peak at 990 °C in the DTA curve could also be attributed to this process [27].

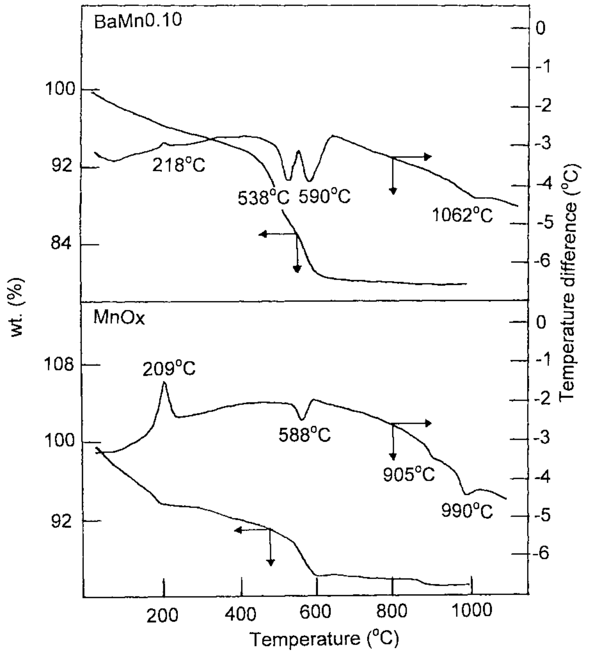

Figure 5. TG-DTA analysis of MnO_2 precursor and Ba-modified BaMn0.10 dried at 110 °C.

Compared with the MnO_2 precursor, the thermal behavior of $Ba(NO_3)_2$ impregnated MnO_2 is similar, while some differences are also apparent. No evident weight loss is observed from ambient temperature to 450 °C, indicating the lack of big amount of chemically bound water. A much smaller exothermic peak at 218 °C seems to imply that $Ba(NO_3)_2$ can hinder the phase change and the crystallization of MnO_2. The transformations of MnO_2 into Mn_2O_3 and Mn_2O_3 into Mn_3O_4 are also observed in its TG-DTA curves with very similar characteristics to those of the MnO_2 precursor. However, a new fast weight loss step occurs at the temperature region of 450–550 °C, accompanying an obvious endothermic peak at 538 °C. This could be assigned to the reaction between $Ba(NO_3)_2$ and MnO_2, which resulted in the formation of $BaMnO_3$ and $BaMn_8O_{16}$ composite oxides. TG-DTA analysis confirms the XRD results.

3.4. H_2-TPR results

Studies show that a lot of composite metal oxide catalysts contain more mobile oxygen species than the corresponding single components, which may result in the improved oxidation activity of the obtained catalysts. To check if this effect happens upon the addition of Ba into manganese oxide, H_2-TPR was thus used in this study. The results are shown in figure 6.

Two reduction peaks positioned at 350 and 415 °C, respectively, are observed for MnO_x, which are attributed to the reduction of Mn_2O_3, the main component of this catalyst, to MnO with Mn_3O_4 as the intermediate [28,29]. However, for the Ba-modified samples, three reduction peaks are seen in their profiles, with the main peak siting at 420 °C. The other two smaller peaks are positioned at ~300 and 370 °C, respectively. It is worth noting here that the main reduction product of the modified samples could also be MnO, as proved by its green color. Upon increasing the Ba loading, the H_2 consumption of the 420 °C peak increases, as evidenced by the increase of its area. Therefore, this peak may be assigned to the reduction of Mn^{4+} to Mn^{2+} in the lattice of $BaMnO_3$, since XRD shows the amount of this phase also increases with the increase of Ba loading. The assignment of the two low-temperature peaks is not very clear now, while they may be attributed to the overlapped reduction of left Mn_2O_3 together with $BaMn_8O_{16}$ and $BaMnO_3$ in the samples. The sharper and narrower shape of the 420 °C peak indicates that the oxygen species in the modified samples is more uniform. However, H_2-TPR results show that the mobility of the oxygen species in the Ba-modified catalysts is not improved.

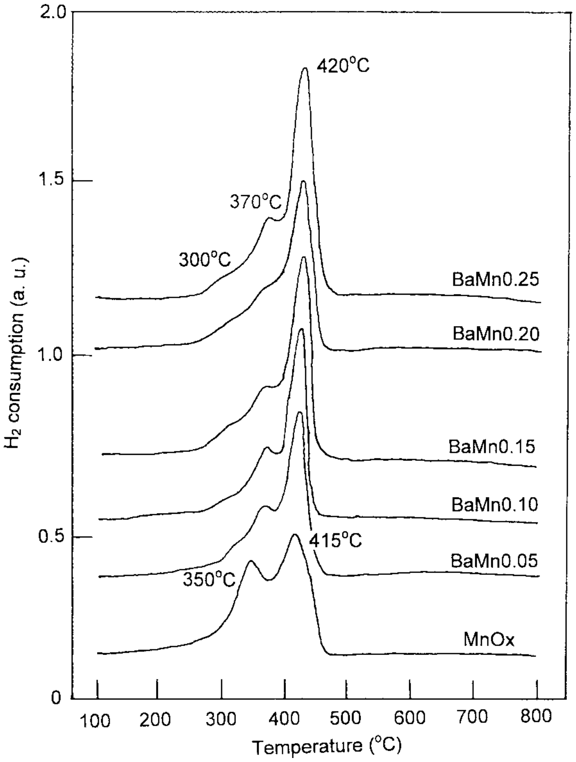

Figure 6. H_2-TPR profiles of the catalysts.

3.5. CH_4-TPR results

In the oxidation of methane, CH_4 molecules are supposed to react first with oxygen species on the catalysts and activated [29]. To get more direct information and understand the effects of Ba addition on the nature of the oxygen species, CH_4-TPR was thus employed to characterize the catalysts, with the results shown in figure 7.

In the CH_4-TPR experiments, the color of the reduction product is also green for all of the samples, indicating that MnO is the main product. Again, two reduction peaks are observed for MnO_x, which locate at 500 and 605 °C, respectively. Since the two peaks do not separate from each other very clearly, it is difficult for us to do some peak de-

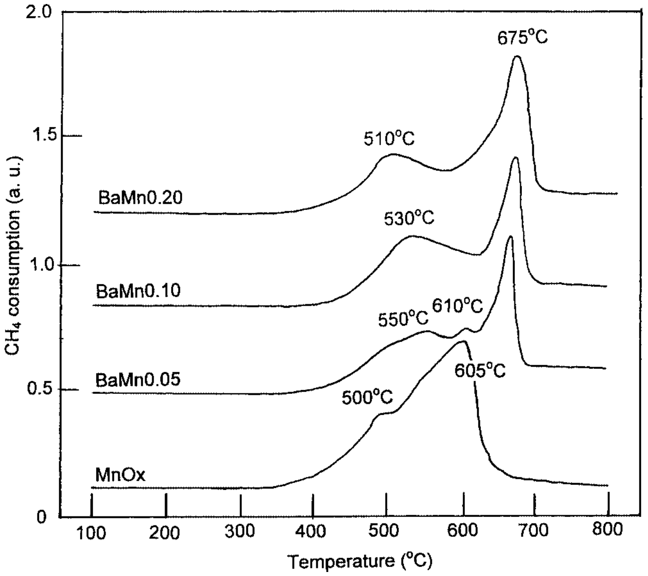

Figure 7. CH_4-TPR profiles of the catalysts.

convolution and quantitative calculation, as in the H_2-TPR case. However, the similar reduction behavior was found by Stobbe et al. [29]; they assigned the two peaks to the reduction of Mn_2O_3 to MnO with Mn_3O_4 as the intermediate. The addition of Ba alters the CH_4 reduction behavior of the catalysts. A new reduction peak siting at ~675 °C appears, whose area increases with the increase of Ba loading. Compared with XRD and H_2-TPR results, this peak is attributed to $BaMnO_3$, a new-formed crystalline phase in the Ba-modified samples. BaMn0.05 still shows somewhat the reduction characteristics of Mn_2O_3, as evidenced by a small reduction peak at 610 °C. However, further increase of Ba loading decreases the amount of Mn_2O_3, and covers its reduction behavior. For all the Ba-modified samples, a reduction peak at lower temperature is also found in their profiles. The temperature of this peak decreases from 550 to 510 °C upon increasing Ba/Mn mol ratio from 0.05 to 0.20.

It is noticed that the addition of Ba makes the reduction happen generally at higher temperature. Therefore, CH_4-TPR confirms the results of H_2-TPR, which shows that the addition of Ba does not improve the mobility of the oxygen species in the achieved samples.

4. Discussion

In this work, it is evident that the addition of a suitable amount of Ba significantly enhances the activity of manganese oxide toward CH_4 deep oxidation. The optimal Ba/Mn mol ratio is ~0.10. Previously, Zaki et al. [25] substantiated that the alkalization of Mn_2O_3 by K or Ba can improve the electron density and the mobility of its lattice and surface oxygen species, thus leading to the promoted activity of the obtained catalysts for H_2O_2 decomposition. In contrast, similar to this study, they found that the CO oxidation activity of manganese oxide is not improved by the alkalization, but maintained.

It is reported that CH_4 oxidation over metal oxide catalysts, such as perovskites [31] and manganese oxide [29], proceeds via a Mars–Van Krevelen mechanism. This could also be true for CO oxidation over manganese oxide catalysts. Based on this mechanism, the catalysts undergo a redox cycle during the reactions. The redox process in this study is supposed to proceed between Mn^{3+} and Mn^{4+}, since these two oxidation states are found to be stable in the catalysts.

In the unmodified MnO_x, the main component is α-Mn_2O_3, together with a trace amount of β-MnO_2. Obviously, the predominant oxidation state of Mn is 3+. Upon adding Ba into manganese oxide, a considerable amount of Mn was stabilized in the lattice of $BaMnO_3$ and $Ba_2Mn_8O_{16}$ at the oxidation state of 4+. In these samples, α-Mn_2O_3 is also present, as testified by XRD and evidenced by TG-DTA results. The coexistence of both Mn^{3+} and Mn^{4+} in the modified samples may devote to the enhanced CH_4 oxidation activity of them, since the electron transfer between Mn with different oxidation states could happen without the ions changing their positions, and thus become easier [27,32]. However, the CO oxidation activity of the modified samples is not improved. Therefore, we speculate that some other reasons may be more crucial for the enhanced CH_4 oxidation activity of the modified catalysts.

Kung et al. [33] demonstrated that both lattice oxygen and dissociatively adsorbed surface oxygen can contribute to deep oxidation of hydrocarbons. On studying CO oxidation over Ag-modified manganese oxide catalysts, Imamura et al. [16,17] and Luo et al. [18] observed the stabilization of Ag as oxidized form by the presence of manganese oxides. Since the Ag–O bond is weak and its oxygen is readily to be removed, they thus proposed that Ag ions play the role as active sites to oxidize CO. Then, the reduced Ag^0 is reoxidized by obtaining oxygen from manganese oxides. Due to the cooperative action between Ag and Mn, the CO oxidation activity of Ag-modified manganese oxides is markedly enhanced. However, when studying Ag/MnO_x/perovskite catalysts for CO oxidation, Song et al. [19] attributed the improved CO oxidation activity of the catalysts to the formation of a great amount of weakly adsorbed oxygen species by Ag addition. A common opinion of these authors is that the presence of more mobile and reactive oxygen species is crucial for the CO oxidation activity of the catalysts, which is able to increase the rates of the overall reaction remarkably. In this study, there is no proof to show the presence of detectable amount of weakly adsorbed oxygen species in the modified catalysts, as evidenced by the lack of a low-temperature reduction peak in their H_2-TPR and CH_4-TPR profiles. Furthermore, compared with the unmodified MnO_x, the reactivity of the lattice oxygen of the modified samples is also not improved, but decreased a little. This could be the main reason why the CO oxidation activity of the modified catalysts is not promoted by the addition of Ba.

CH_4 is well known to be the most difficult to oxidize among all the hydrocarbons, since its molecule contains only very potent C–H bonds [1]. The rupture of the first

C–H bond is commonly regarded as the rate-determining step for CH_4 oxidation, and generally occurs at high temperature [7–13]. This may be the main difference between CO and CH_4, since the former can be activated much more easily than the latter. Indeed, the much higher activation energy for CH_4 oxidation than that for CO oxidation found in current work confirms this. When studying CH_4 oxidative coupling, Campbell et al. [13] found that the relative activity of rare-earth metal oxides parallels their basicity. They pointed out that this could be due to the better ability of more basic metal oxide to abstract one hydrogen atom from a CH_4 molecule to form a methyl radical, the important reaction intermediate. Most recently, it is also suggested that for efficient activation of CH_4 in combustion, highly basic sites are required in a catalyst [8]. Previous work has already demonstrated that Ba addition into manganese oxides can improve the basicity of their lattice oxygen [25]. We thus postulate that in this study, the predominant reason leading to the enhanced CH_4 oxidation activity of the Ba-modified manganese oxide catalysts, actually, could be attributed to their improved basicity, which is favorable for the activation of C–H bonds in CH_4.

However, figure 3 shows that the CH_4 oxidation activity of the catalysts does not always rise with the increase of Ba loading. The addition of too much Ba, conversely, suppresses the activity. This may be due to the lowering of the mobility of the lattice oxygen because of the formation of $BaMnO_3$ and $BaMn_8O_{16}$ in the samples, as evidenced by CH_4-TPR and H_2-TPR results. In other words, the promoted C–H bond activation ability of the catalysts could be offset by the decreased mobility of the lattice O^{2-} at high Ba loading, thus resulting in the lower CH_4 oxidation activity.

5. Conclusion

In summary, the addition of a suitable amount of Ba into manganese oxide can improve its activity toward CH_4 oxidation. The most active catalyst is achieved with Ba/Mn atomic ratio around 0.1. Whereas, this promotion effect is not observed for CO oxidation over the Ba-modified catalysts.

As to CO oxidation, the activation of CO is easy and the reactivity of the oxygen species in the catalysts is crucial for the overall reaction. However, this factor is not so critical for CH_4 oxidation as for CO oxidation. Generally, since the rupture of the first C–H bond in CH_4 is very difficult, it is considered as the rate-determining step. In this study, characterization results show that the reactivity of the oxygen species is not improved by the addition of Ba, whereas, the basicity of the modified catalysts could be improved, which is believed to be favorable to activate C–H bonds in CH_4. It is thus concluded that due to this modification effect of Ba, the CH_4 oxidation activity of the Ba-modified catalysts is enhanced, while the CO oxidation activity of them remains unchanged.

Acknowledgement

Financial support from the National Science Foundation of China is greatly acknowledged by the authors.

References

[1] Y. Li and J.N. Armor, Appl. Catal. B 3 (1994) 275.
[2] W.S. Epling and G.B. Hoflund, J. Catal. 182 (1999) 5.
[3] Lj. Kundakovic and M. Flytzani-Stephanopoulos, Appl. Catal. A 183 (1999) 35.
[4] E.S. Rubin, R.N. Cooper, R.A. Frosch, T.H. Lee, G. Marland, A.H. Rosenfield and D.D. Stine, Science 257 (1992) 148.
[5] L.D. Pfefferle and W.C. Pfefferle, Catal. Rev. Sci. Eng. 29 (1987) 219.
[6] M.M. Zwinkel, S.G. Jaras and P.C. Menon, Catal. Rev. Sci. Eng. 35 (1993) 319.
[7] M.I. Zaki, M.A. Hasan, L. Pasupulety, N.E. Fouad and H. Knözinger, New J. Chem. (1999) 1197.
[8] R. Burch, D.J. Crittle and M.J. Hayes, Catal. Today 47 (1999) 229.
[9] J. Au-Yeung, K. Chen, A.T. Bell and E. Iglesia, J. Catal. 188 (1999) 132.
[10] K. Fujimoto, F.H. Ribeiro, M. Avalos-Borja and E. Iglesia, J. Catal. 179 (1998) 431.
[11] Lj. Kundakovic and M. Flytzani-Stephanopoulos, J. Catal. 179 (1999) 203.
[12] V.R. Choudhary and V.H. Rane, J. Catal. 130 (1991) 411.
[13] K.D. Campbell, H. Zhang and J.H. Lunsford, J. Phys. Chem. 92 (1988) 750.
[14] R. Doshi, C.B. Alcock, N. Gunasekaran and J.J. Carbery, J. Catal. 140 (1993) 557.
[15] M. Shelef and G.W. Graham, Catal. Rev. Sci. Eng. 36 (1994) 433.
[16] S. Imamura, H. Sawada, K. Uemura and S. Ishida, J. Catal. 109 (1988) 198.
[17] S. Imamura and S. Yoshie, J. Catal. 115 (1989) 258.
[18] M.-F. Luo, X.-X. Yuan and X.-M. Zheng, Appl. Catal. A 175 (1998) 121.
[19] K.-S. Song, S.-K. Kang and S.D. Kim, Catal. Lett. 49 (1997) 65.
[20] Z. Jaworska-Galas, W. Mista, J. Wrzyszcz and M. Zawadzki, Catal. Lett. 24 (1994) 133.
[21] M. Baldi, V.S. Escribano, J.M.G. Amores, F. Milella and G. Busca, Appl. Catal. B 17 (1998) L175.
[22] D. Mehandjiev, E. Zhecheva, G. Ivanov and R. Ioncheva, Appl. Catal. A 167 (1998) 277.
[23] T. Yamashita and A. Vannice, Appl. Catal. B 13 (1997) 141.
[24] R. Burch, S. Chalker, G.D. Squire and S.C. Tsang, J. Chem. Soc. Faraday Trans. 86 (1990) 1607.
[25] M.I. Zaki, M.A. Hasan, L. Pasupulety, N.E. Fouad and K. Kumari, New J. Chem. (1998) 875.
[26] E.C. Pitzer and J.C.W. Frazer, J. Phys. Chem. 45 (1941) 761.
[27] S.B. Kanungo, J. Catal. 58 (1979) 419.
[28] X. Wang and Y.C. Xie, React. Kinet. Catal. Lett. 70 (2000) 43.
[29] E.R. Stobbe, B.A. De Boer and J.W. Geus, Catal. Today 47 (1999) 161.
[30] R. Metselaar, R.E.J. Van Tol and P. Piercy, J. Solid State Chem. 38 (1981) 335.
[31] H. Arai, T. Yamada, K. Eguchi and T. Seiyama, Appl. Catal. 26 (1986) 265.
[32] G.M. Schwab and S.B. Kanungo, Z. Physik. Chem. NF 107 (1977) 109.
[33] H. Kung and M. Kung, Adv. Catal. 33 (1984) 159.